

Coulomb blockage of hybridization in two-dimensional DNA arraysArnold Vainrub* and B. Montgomery Pettitt*[†]*Department of Chemistry, University of Houston, Houston, Texas 77204-5003*

(Received 23 April 2002; published 17 October 2002)

Experiments on DNA microarrays have revealed substantial differences in hybridization thermodynamics between DNA free in solution and surface tethered DNA. Here we develop a mean field model of the Coulomb effects in two-dimensional DNA arrays to understand the binding isotherms and thermal denaturation of the double helix. We find that the electrostatic repulsion of the assayed nucleic acid from the array of DNA probes dominates the binding thermodynamics, and thus causes the Coulomb blockage of the hybridization. The results explain, observed in DNA microarrays, the dramatic decrease of the hybridization efficiency and the thermal denaturation curve broadening as the probe surface density grows. We demonstrate application of the theory for evaluation and optimization of the sensitivity, specificity, and the dynamic range of DNA array devices.

DOI: 10.1103/PhysRevE.66.041905

PACS number(s): 87.14.Gg, 87.15.Rn

Broad interest in DNA arrays and their growing use in computing, genetics, medicine, and drug discovery [1] is connected with their ability to perform massive parallel sequence analyses of polymeric nucleic acid. DNA microarrays were introduced as a revolutionary technological development of solution hybridization assays based on formation of a double helix to a surface immobilized single-strand DNA probe according to Watson-Crick pairing rules. In a single-microarray experiment, the hybridization is performed with up to hundreds of thousands of different probes producing tremendous volume of information on the assayed polymeric DNA sequence strings and their abundance in tested target. Typically, a DNA microarray contains 10^7 – 10^{10} DNA probe molecules of each sequence to be tested immobilized in a ~ 50 - μm -diameter spot on a prepared glass surface, and thus may include about 10^4 – 10^5 different probe spots per cm^2 . Usually, the probes are oligonucleotides of 8–80 bases long, tethered by one end through a linker molecule to the surface. DNA microbeads are similar to microarrays, but the probes are tethered to a micron size glass bead surface [2].

Experiments on DNA arrays have revealed substantial differences in hybridization thermodynamics of DNA free in solution and surface tethered DNA. The main observations include a considerable decrease in the thermodynamic stability of the DNA duplex on the surface with a concomitant suppression of the thermal denaturation temperature of the duplex into single strands and a dramatic broadening of the thermal denaturation (duplex melting) curve [3–5]. Recent, more detailed experiments demonstrated that these effects grow as the surface density of probes increases [6,7]. Although for common experimental conditions these phenomena can adversely affect the DNA array performance by suppression of the sensitivity and ability to detect mutations, they are not well understood. In contrast to a large experimental effort, the theoretical analysis of DNA arrays [8] has got much less attention. We previously considered the effect

of the nucleic acid–surface electrostatic interaction on the thermodynamics of the surface hybridization [9,10]. This theory used an analytical solution of the linearized Poisson-Boltzmann boundary value problem for a charged sphere-surface interaction in electrolyte solution, and corresponds to the system characterized by a low surface density of immobilized probes. In this paper, we focus on different types of electrostatic interactions in DNA arrays, namely on the repulsion between the immobilized probe layer, and on the assayed DNA. We show this interaction to dominate the binding phenomena and accounts for observed hybridization thermodynamics in DNA arrays on both glass and gold.

Consider formation of duplex (D) DNA by hybridization of the dissolved nucleic acid target (T) with the surface tethered DNA probe (P). As the target concentration C is kept constant, this reversible reaction obeys first-order kinetics, and thus the hybridization yield θ ($0 < \theta < 1$) at equilibrium is given by [11]

$$\theta = \frac{1}{1 + C^{-1} \exp(\Delta G/kT)}. \quad (1)$$

where $\Delta G = \Delta H - T\Delta S$ is the duplex binding Gibbs free energy; ΔH and ΔS are the binding enthalpy and entropy, respectively. As the binding free energy ΔG is independent of θ , Eq. (1) corresponds to the well-known Langmuir adsorption isotherm. Here, to account for the screened electrostatic repulsion of the target from the probe array, we introduce the Gibbs free energies of interaction V_D , V_P , and V_T for the duplex, probe, and target, respectively. The interaction shifts the binding energy ΔG by $(V_D - V_P - V_T)$, and thus

$$\Delta G = \Delta G_0 + V_D - V_P - V_T, \quad (2)$$

where ΔG_0 is the binding free energy for low probe surface density when the repulsion is negligibly small. In addition, the repulsion $V_T > 0$ depletes targets near the probe array according to

$$C = C_0 \exp(-V_T/kT). \quad (3)$$

Substitution of Eqs. (2) and (3) into Eq. (1) gives

*FAX: 713-743-2709. Email address: vainrub@uh.edu, pettitt@uh.edu

[†]Email address: pettitt@uh.edu

$$\theta = \frac{1}{1 + C_0^{-1} \exp[(\Delta G_0 + V_D - V_P)/kT]}. \quad (4)$$

We evaluate the free energies V_D and V_P in a model similar to our recent calculation of DNA electrostatic interaction with charged metallic and dielectric surfaces in electrolyte solution [10]. There we used the exact analytical solution of the linearized Poisson-Boltzmann (PB) equation for a charged ion-penetrable sphere near the solution-solid interface obtained by Ohshima and Kondo [12]. In the present case, the linearized PB equation and the boundary conditions are

$$\Delta \phi = \kappa^2 \phi, \quad \text{outside the sphere and plane,}$$

$$\Delta \phi = \kappa^2 \phi - (\rho/\epsilon \epsilon_0), \quad \text{inside the sphere,}$$

$$\phi|_{r=a+} = \phi|_{r=a-}, \quad \partial_r \phi|_{r=a+} = \partial_r \phi|_{r=a-}, \quad \text{on the sphere,}$$

$$\phi|_{z=0+} = \phi|_{z=0-},$$

$$\partial_z \phi|_{z=0+} - \partial_r \phi|_{z=0-} = -\sigma/\epsilon \epsilon_0, \quad \text{on the plane.} \quad (5)$$

Here $1/\kappa = (\epsilon \epsilon_0 kT/2n_0 e^2)^{1/2}$ is the Debye screening length for the relevant case of a monovalent electrolyte at concentration n_0 , ρ is the local charge density inside the sphere of radius a , and σ is the surface charge density on the plane located at $z=0$. This boundary value problem is similar to the one solved by Ohshima and Kondo [12], but differs in the on-plane boundary condition. We solve it by the same method [10,12] and obtain the free energy of interaction [13],

$$V(h) = \frac{2\pi a \sigma \phi_{s0} \exp(-\kappa h)}{\kappa}, \quad (6)$$

where h is the distance between the sphere surface and plane, and ϕ_{s0} is the unperturbed potential on the sphere's surface, which for an isotropic charge density $\rho(r)$ is given by

$$\phi_{s0} = \frac{\exp(-\kappa a)}{\epsilon \epsilon_0 \kappa a} \int_0^a r \rho(r) \sinh(\kappa r) dr. \quad (7)$$

Importantly, the repulsion $V(h)$ in Eq. (6) increases as the hybridization proceeds because the charge of hybridized targets contributes to σ . Indeed, $\sigma = eZN_P(1 + \theta)$, where N_P is the surface density of probes, Z is the probe length (the number of bases), and for simplicity, the target length is assumed to be the same. Therefore,

$$V_D - V_P = V_s Z N_P (1 + \theta), \quad (8)$$

where

$$V_s = 2\pi e (a_D \phi_{D0} - a_P \phi_{P0}) / \kappa \quad (9)$$

corresponds to a probe- and duplex-surface distance $h=0$ in Eq. (6). Substitution of Eq. (8) in Eq. (4) gives the hybridization adsorption isotherm

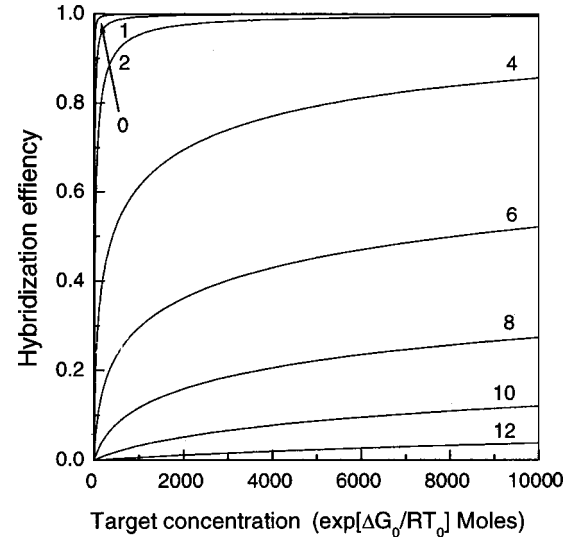


FIG. 1. Hybridization binding isotherm at different surface density of 25-mer probe oligonucleotides. The curve number notes the surface density in 10^{12} probes/cm² units. The number zero corresponds to the Langmuir isotherm.

$$C = \frac{\theta}{1 - \theta} \exp\left(\frac{\Delta G_0}{kT}\right) \exp\left[\frac{V_s Z N_P (1 + \theta)}{kT}\right]. \quad (10)$$

This isotherm differs from the Langmuir isotherm, Eq. (1), by the factor $\exp[V_s Z N_P (1 + \theta)/kT]$, which accounts for repulsion of the assayed DNA from the probe layer.

How strong are these electrostatic repulsion effects in DNA microarrays? To answer the question we estimate the interaction V_s . As we suggested previously [10], the short eight-base-pair DNA double helix of diameter 2 nm and height 2.4 nm is modeled by a 1-nm-radius sphere. At typical 1M NaCl concentration, the Debye screening length is $1/\kappa = 0.3$ nm, and according to Eq. (7) the sphere's potential is $\phi_{s0} = -14$ mV for uniformly distributed charge $-8e$. Thus Eq. (9) gives $V_s = 2.6 \times 10^{-15}$ J m²/mol for eight-pair length. Assuming linear scaling, this value is interpolated to 8×10^{-15} for a typical DNA microarray with probe oligonucleotides 25 bases long. Although the model simplifies the repulsion of DNA inserted into the probe layer as a screened charged sphere-plane interaction, this value is rather consistent with independent V_s estimates described below from the experimental data.

Figure 1 shows the hybridization binding isotherm $\theta = \theta(C)$ at different probe surface densities. The curves are calculated from Eq. (10) at room temperature, and typical DNA array parameters $Z = 25$, $V_s = 10^{-14}$ J m²/mol. Decrease of the hybridization efficiency in Fig. 1 with the probe density is connected with the electrostatic repulsion increase, as the total density of probes (charge) grows as discussed above. Interestingly, the decline from the Langmuir isotherm (curve for $N_P = 0$) and suppression of hybridization start already at a probe surface density of 10^{12} cm⁻² corresponding to a mean interprobe distance of 10 nm, which is large compared to the DNA helix diameter of 2 nm. Thus the electrostatic repulsion appears at lower probe densities compared to

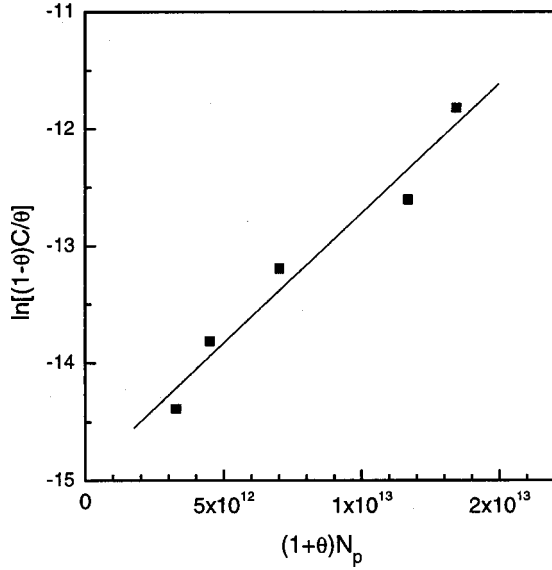


FIG. 2. Linear fit by Eq. (11) of the experimental data [7].

steric restrictions that become effective as the helices start to overlap. The above theoretical results give a consistent explanation of experiments [7] on hybridization with 25-base oligonucleotide probes at different probe surface densities from 2×10^{12} to 1.2×10^{13} cm^{-2} . Figure 2 demonstrates the fit of the experimental data by Eq. (10), rewritten as

$$kT \ln \left[\frac{C(1-\theta)}{\theta} \right] = V_s Z N_p (1+\theta) + \Delta G_0. \quad (11)$$

In accord with our theory, the experimental points follow the linear $\ln[C(1-\theta)/\theta]$ vs $N_p(1-\theta)$ dependence with a slope corresponding to $V_s = 2.5 \times 10^{-15}$ $\text{J m}^2/\text{mol}$. This value should be taken with caution because the data in Ref. [7] are for a 30-min reaction time when the hybridization may not have fully achieved equilibrium.

The temperature dependence of equilibrium hybridization determines the hybridization temperature to optimize the sensitivity and selectivity of the hybridization assay. In Fig. 3 we present the melting curves $\theta(T)$ at different probe surface densities N_p calculated from Eq. (10). We took the parameters $\Delta H_0 = -608.2$ kJ mol^{-1} and $\Delta S_0 = -1.729$ $\text{kJ mol}^{-1} \text{K}^{-1}$ (Ref. [14]), $n_0 = 1\text{M}$ NaCl, $C_0 = 0.1$ μM corresponding to an experimentally studied 20-mer helix dA_{20}/dT_{20} (Ref. [6]). The remarkable result is the prominent suppression of the melting temperature and broadening of the melting curve as the probe surface density increases. This prediction is in complete accord with numerous experiments [3–7] and provides a basis for their understanding. Physically, in our picture, the target-probe layer repulsion causes the Coulomb blockage of hybridization, and thus decreases the melting temperature. In addition, since the repulsion increases with the number of hybridized targets, the melting curve becomes broader. Quantitatively, from Eq. (10) we get for the melting temperature shift ΔT_m and additional broadening ΔW ,

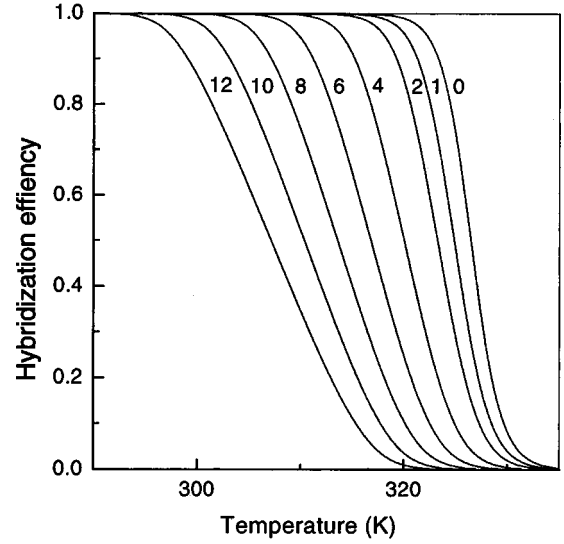


FIG. 3. Melting curves for dA_{20}/dT_{20} duplexes at different densities of the probe oligonucleotides dT_{20} . The curve number notes the surface density in 10^{12} probes/ cm^2 units.

$$\Delta T_m = \frac{3V_s Z N_p}{2\Delta H_0 + 3V_s Z N_p}, \quad \Delta W = \frac{2}{3} \Delta T_m. \quad (12)$$

Here both the melting temperature T_m and width of the melting curve $W = dT/d\theta$ are defined at the middle point $\theta = 1/2$. Experimentally, in Ref. [6], $\Delta T_m = -8.5$ K for a perfect match dA_{20}/dT_{20} and -12 K for the duplex with a single mismatch $d(A_9GA_{10}/dT_{20})$ at $N_p = 4.6 \times 10^{12}$ cm^{-2} . We use these two results to make two estimates, which are similar (within 15% range) and average to $V_s = 1.1 \times 10^{-14}$ $\text{J m}^2/\text{mol}$. This value supports the above theoretical estimate of 8×10^{-15} $\text{J m}^2/\text{mol}$.

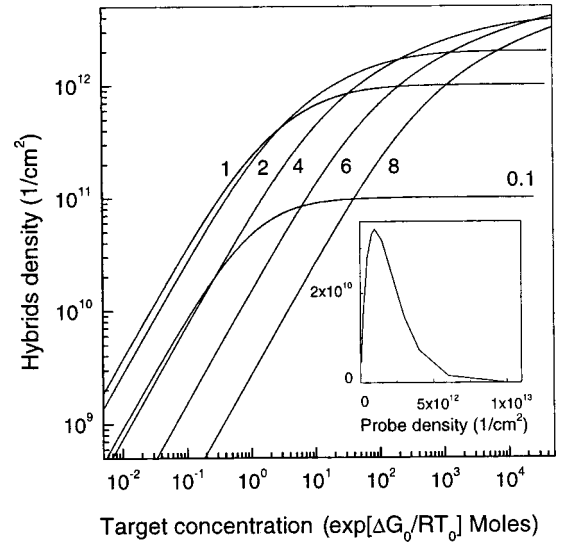


FIG. 4. Number of hybridized probes as a function of the normalized target concentration at different surface density of 25-mer probe oligonucleotides. The curve number notes the surface density in 10^{12} probes/ cm^2 units. The inset shows the number of hybrids vs probe surface density at the normalized target concentration of 0.1.

Next, we consider the effect of the Coulomb blockage on the sensitivity and dynamic range of DNA microarrays. Figure 4 shows the number of hybrids θN_p as a function of the target concentration at different probe densities N_p assuming the same array parameters $Z=25$, $V_s=10^{-14}$ J m²/mol, and room temperature $T=298$ K as in Fig. 1. For microarray assays in the low target concentration regime, the strongest signals correspond to a probe density of about 10^{12} cm⁻². As seen in the inset of Fig. 4, the sensitivity peak is rather narrow, suggesting that the probe density in microarrays should be thoroughly optimized. This result is in accord with experimental observations of a clear signal peak in a similar probe density range [15], and a weaker signal at higher probe densities [7]. Figure 4 shows that the dynamic range near higher target concentrations can be expanded by an increase of the probe density at expense of a substantial decrease in sensitivity.

Explicit control of the electrostatic interactions is therefore of obvious importance for optimization of microarrays. Under the operating conditions of those devices, suppression of the Coulomb repulsion increases the sensitivity. We expect that this could be achieved using external fields, charged molecular surface preparations, and in three-dimensional

(3D) arrays using probe immobilization in gels, which indeed show solutionlike hybridization thermodynamics [16] but suffer from the slow hybridization and washing kinetics. For 2D arrays, use of multivalent counterions for enhancement of the Coulomb screening, repulsion reduction [17], as well as the use of a positive electrostatic potential at the surface [10] may be important. In addition, replacement of DNA probes by noncharged peptide nucleic acids (Ref. [18]) provides an interesting chemical way to lessen the unfavorable electrostatic interaction. It should be noted that the Coulomb repulsion can play a positive role in 2D hybridization experiments, such as in the case for single-nucleotide polymorphism genotyping. Here simultaneous detection of mutations in a number of genes demands overlap in the temperature range of their melting curves. Increasing the melting curve width by increase of the probe surface density or decrease of the hybridization solution ionic strength can achieve this by our analysis.

The authors thank Professor R. Georgiadis, Professor M. Hogan, Professor B. I. Shklovskii, and Dr. R. Mitra for discussions. This work was partially supported by a grant from the National Institutes of Health and by the Robert A. Welch Foundation.

-
- [1] See reviews in the special issue: Chipping Forecast. *Nature Genet.* **21**, (1999).
- [2] S. Brenner *et al.*, *Nat. Biotechnol.* **18**, 630 (2000).
- [3] Z. Guo *et al.*, *Nucleic Acids Res.* **22**, 5456 (1994).
- [4] M. S. Shchepinov, S. C. Case-Green, and E. M. Southern, *Nucleic Acids Res.* **25**, 1155 (1995).
- [5] J. E. Forman *et al.*, *ACS Symp. Ser.* **682**, 206 (1998).
- [6] J. H. Watterson *et al.*, *Langmuir* **16**, 4984 (2000).
- [7] A. W. Peterson, R. J. Heaton, and R. M. Georgiadis, *Nucleic Acids Res.* **29**, 5163 (2001).
- [8] V. Chan, D. J. Graves, and S. E. McKenzie, *Biophys. J.* **69**, 2243 (1995).
- [9] A. Vainrub and B. M. Pettitt, *Biopolymers* (to be published).
- [10] A. Vainrub and B. M. Pettitt, *Chem. Phys. Lett.* **323**, 160 (2000).
- [11] R. Alberty, *Physical Chemistry* (Wiley, New York, 1992).
- [12] H. Ohshima and T. Kondo, *J. Colloid Interface Sci.* **157**, 504 (1993).
- [13] The second image interaction term discussed in Ref. [10] vanishes for the present boundary conditions where an electrolyte solution fills all the space around the probe layer.
- [14] J. SantaLucia, H. T. Allawi, and P. A. Seneviratne, *Biochemistry* **35**, 3555 (1996).
- [15] A. B. Steel, T. M. Herne, and M. J. Tarlov, *Anal. Chem.* **70**, 4670 (1998).
- [16] V. A. Vasiliskov, D. V. Prokopenko, and A. D. Mirzabekov, *Nucleic Acids Res.* **29**, 2303 (2001).
- [17] T. T. Nguyen, A. Y. Grosberg, and B. I. Shklovskii, *J. Chem. Phys.* **113**, 1110 (2000).
- [18] P. E. Nielsen, *Curr. Opin. Biotechnol.* **12**, 16 (2001).